

PROCEEDINGS OF SPIE

Image and Signal Processing for Remote Sensing XX

**Lorenzo Bruzzone
Jon Atli Benediktsson
Francesca Bovolo**
Editors

**22–24 September 2014
Amsterdam, Netherlands**

Sponsored by
SPIE

Cooperating Organisations
European Association of Remote Sensing Companies (Belgium)
Remote Sensing and Photogrammetry Society (United Kingdom)
European Optical Society
CENSIS—Innovation Centre for Sensor & Imaging Systems
EUFAR—European Facility for Airborne Research
EARSeL—European Association of Remote Sensing Laboratories
TNO
ESA

Published by
SPIE

Volume 9244

Proceedings of SPIE 0277-786X, V. 9244

SPIE is an international society advancing an interdisciplinary approach to the science and application of light.

Image and Signal Processing for Remote Sensing XX, edited by Lorenzo Bruzzone, Jon Atli Benediktsson,
Francesca Bovolo · Proc. of SPIE Vol. 9244, 924401 · © 2014 SPIE
CCC code: 0277-786X/14/\$18 · doi: 10.1117/12.2177855

Proc. of SPIE Vol. 9244 924401-1

The papers included in this volume were part of the technical conference cited on the cover and title page. Papers were selected and subject to review by the editors and conference program committee. Some conference presentations may not be available for publication. The papers published in these proceedings reflect the work and thoughts of the authors and are published herein as submitted. The publisher is not responsible for the validity of the information or for any outcomes resulting from reliance thereon.

Please use the following format to cite material from this book:

Author(s), "Title of Paper," in *Image and Signal Processing for Remote Sensing XX*, edited by Lorenzo Bruzzone, Jon Atli Benediktsson, Francesca Bovolo, Proceedings of SPIE Vol. 9244 (SPIE, Bellingham, WA, 2014) Article CID Number.

ISSN: 0277-786X

ISBN: 9781628413076

Published by

SPIE

P.O. Box 10, Bellingham, Washington 98227-0010 USA

Telephone +1 360 676 3290 (Pacific Time) · Fax +1 360 647 1445

SPIE.org

Copyright © 2014, Society of Photo-Optical Instrumentation Engineers.

Copying of material in this book for internal or personal use, or for the internal or personal use of specific clients, beyond the fair use provisions granted by the U.S. Copyright Law is authorized by SPIE subject to payment of copying fees. The Transactional Reporting Service base fee for this volume is \$18.00 per article (or portion thereof), which should be paid directly to the Copyright Clearance Center (CCC), 222 Rosewood Drive, Danvers, MA 01923. Payment may also be made electronically through CCC Online at copyright.com. Other copying for republication, resale, advertising or promotion, or any form of systematic or multiple reproduction of any material in this book is prohibited except with permission in writing from the publisher. The CCC fee code is 0277-786X/14/\$18.00.

Printed in the United States of America.

Publication of record for individual papers is online in the SPIE Digital Library.



SPIDigitalLibrary.org

Paper Numbering: Proceedings of SPIE follow an e-First publication model, with papers published first online and then in print and on CD-ROM. Papers are published as they are submitted and meet publication criteria. A unique, consistent, permanent citation identifier (CID) number is assigned to each article at the time of the first publication. Utilization of CIDs allows articles to be fully citable as soon as they are published online, and connects the same identifier to all online, print, and electronic versions of the publication. SPIE uses a six-digit CID article numbering system in which:

- The first four digits correspond to the SPIE volume number.
- The last two digits indicate publication order within the volume using a Base 36 numbering system employing both numerals and letters. These two-number sets start with 00, 01, 02, 03, 04, 05, 06, 07, 08, 09, 0A, 0B ... 0Z, followed by 10-1Z, 20-2Z, etc.

The CID Number appears on each page of the manuscript. The complete citation is used on the first page, and an abbreviated version on subsequent pages. Numbers in the index correspond to the last two digits of the six-digit CID Number.

Contents

- vii *Authors*
- ix *Conference Committee*
- xi *Remote sensing at the NASA Kennedy Space Center and the Eastern Range: a perspective from the ground up (Plenary Paper) [9241-100]*

VHR IMAGE ANALYSIS AND FUSION

- 9244 02 **Full-scale assessment of pansharpening methods and data products [9244-1]**
- 9244 03 **Methods and metrics for the assessment of Pan-sharpening algorithms [9244-2]**
- 9244 04 **A method for generating high-resolution satellite image time series [9244-3]**
- 9244 05 **Spatial resolution enhancement of hyperspectral image based on the combination of spectral mixing model and observation model [9244-5]**

IMAGE SEGMENTATION

- 9244 06 **Efficient hyperspectral image segmentation using geometric active contour formulation [9244-6]**
- 9244 07 **A fuzzy segmentation tool for remote sensing data [9244-7]**
- 9244 08 **Automatic large-volume object region segmentation in lidar point clouds [9244-8]**
- 9244 09 **Edge-crease detection and surface reconstruction from point clouds using a second-order variational model [9244-9]**
- 9244 0A **Three-dimensional building roof boundary extraction using high-resolution aerial image and lidar data [9244-10]**

GEOMETRIC CORRECTIONS AND CO-REGISTRATION

- 9244 0B **SENTINEL-2: geometric calibration during commissioning phase [9244-11]**
- 9244 0C **Automatic registration of multispectral images through maximization of mutual information [9244-12]**
- 9244 0D **On resampling algorithms for the Meteosat Third Generation rectification: feasibility study for an operational implementation [9244-13]**

CALIBRATION, RESTORATION, AND COMPRESSION

- 9244 0F **Image structure restoration from sputnik with multi-matrix scanners** [9244-17]
- 9244 0H **Prediction of optimal operation point existence and parameters in lossy compression of noisy images** [9244-19]
- 9244 0I **Characteristics analysis of infrared polarization for several typical artificial objects** [9244-20]

FEATURE SELECTION AND CLASSIFICATION

- 9244 0J **Feature selection of hyperspectral data by considering the integration of genetic algorithms and particle swarm optimization** [9244-21]
- 9244 0K **Classification of ocean surface slicks in hybrid-polarimetric SAR data** [9244-22]
- 9244 0O **Automatic outlier suppression for rigid coherent point drift algorithm** [9244-14]

CLASSIFICATION AND ANALYSIS OF URBAN AREAS

- 9244 0P **Urban land-cover classification based on airborne hyperspectral data and field observation** [9244-26]
- 9244 0Q **Fusion of aerial images with mean shift-based upsampled elevation data for improved building block classification** [9244-27]
- 9244 0S **Urban road extraction based on shadow removal and road clues detection from high resolution RGB aerial image** [9244-29]
- 9244 0T **Very fast road database verification using textured 3D city models obtained from airborne imagery** [9244-30]

ANALYSIS OF HYPERSPECTRAL DATA

- 9244 0U **Noise estimation for hyperspectral imagery using spectral unmixing and synthesis** [9244-31]
- 9244 0V **Visibility improvement of shadow regions using hyperspectral band integration** [9244-32]
- 9244 0X **Subspace based non-parametric approach for hyperspectral anomaly detection in complex scenarios** [9244-34]

CHANGE DETECTION AND ANALYSIS OF MULTITEMPORAL IMAGES

- 9244 0Z **Hyperspectral anomalous change detection in the presence of non-stationary atmospheric/illumination conditions** [9244-37]
- 9244 10 **Change detection in very high resolution multisensor optical images** [9244-38]
- 9244 11 **Cloud masking of multitemporal remote sensing images** [9244-39]

ESTIMATION AND DETECTION

- 9244 12 **A semisupervised support vector regression method to estimate biophysical parameters from remotely sensed images** [9244-41]
- 9244 13 **Automatic localization of backscattering events due to particulate in urban areas** [9244-42]
- 9244 14 **Procedure to detect impervious surfaces using satellite images and light detection and ranging (lidar) data** [9244-43]
- 9244 15 **A unified algorithm for ship detection on optical and SAR spaceborne images** [9244-44]
- 9244 16 **An improved algorithm for extracting atmospheric motion vectors in cloud-free region from FY-2E thermal infrared imagery** [9244-45]

SAR DATA ANALYSIS I: JOINT SESSION

- 9244 17 **Port surveillance by using co-occurrence matrix on multi-temporal SAR images** [9244-46]
- 9244 18 **An unsupervised approach based on Riemannian metric to change detection on multi-temporal SAR images** [9244-40]

SAR DATA ANALYSIS II: JOINT SESSION

- 9244 19 **Topography estimation using SAR image polarimetry** [9244-48]
- 9244 1A **A Bayesian network approach to perform SAR/InSAR data fusion in a flood detection problem** [9244-49]

ADDITIONAL MANUSCRIPTS

- 9244 1C **Automatic SAR and optical images registration method based on improved SIFT** [9244-100]

POSTER SESSION

- 9244 1D **Usefulness of wavelet-based features as global descriptors of VHR satellite images** [9244-4]
- 9244 1E **A ground control points sampling design method based on smallest singular value** [9244-15]
- 9244 1F **Small target detection based on three-dimensional principal component analysis in hyperspectral imagery** [9244-35]
- 9244 1I **Two-stage subpixel impervious surface coverage estimation: comparing classification and regression trees and artificial neural networks** [9244-52]
- 9244 1K **Precise geometric correction of LANDSAT-8 images based on Kalman filter** [9244-54]

- 9244 1L **Detection and imaging of the moving target using frequency space-time adaptive processing and fractional Fourier transform** [9244-55]
- 9244 1M **A fast 3D image simulation algorithm of moving target for scanning laser radar** [9244-56]
- 9244 1N **Compressive sensing imaging through a drywall barrier at sub-THz and THz frequencies in transmission and reflection modes** [9244-57]
- 9244 1O **Spatial sampling considerations of the CERES (Clouds and Earth Radiant Energy System) instrument** [9244-58]
- 9244 1P **Analysis of discriminants for experimental 3D SAR imagery of human targets** [9244-59]
- 9244 1Q **Infrared radiation scene generation of stars and planets in celestial background** [9244-60]
- 9244 1S **Intermediate grouping on remotely sensed data using Gestalt algebra** [9244-62]
- 9244 1T **Building recognition based on big template in FLIR images** [9244-63]
- 9244 1U **Real-time detection algorithm of moving ground targets based on Gaussian mixture model** [9244-64]
- 9244 1V **Reducing the complexity of the CCSDS standard for image compression decreasing the DWT filter order** [9244-65]
- 9244 1X **Pansharpening of multispectral images using filtering in Fourier domain** [9244-68]
- 9244 1Y **Performance evaluation of supervised change detection tool on DubaiSat-2 multispectral and pansharp images** [9244-70]
- 9244 20 **Detecting changes on coastal primary sand dunes using multi-temporal Landsat imagery** [9244-72]
- 9244 21 **Geometric superresolution by using a two-dimensional orthogonal encoding mask** [9244-74]
- 9244 22 **Spectrally consistent haze removal in multispectral data** [9244-75]

Authors

Numbers in the index correspond to the last two digits of the six-digit citation identifier (CID) article numbering system used in Proceedings of SPIE. The first four digits reflect the volume number. Base 36 numbering is employed for the last two digits and indicates the order of articles within the volume. Numbers start with 00, 01, 02, 03, 04, 05, 06, 07, 08, 09, 0A, 0B...0Z, followed by 10-1Z, 20-2Z, etc.

Abbattista, Cristoforo, 0C
Abramov, Sergey K., 0H
Acito, Nicola, 0X, 0Z
Aiazzi, B., 02
Akoguz, Alper, 1X
Albalooshi, Fatema A., 06
Almatroushi, Hessa R., 1Y
Alonso-Rodríguez, M. C., 14
Alparone, L., 02
Altan, Hakan, 1N
Amorós-López, J., 11
An, Wei, 1E
Arígela, Saibabu, 0V
Arozarena Villar, A., 14
Asari, Vijayan K., 06, 08, 0V
Baraldi, Andrea, 03
Barbré, Robert E., Jr., xi
Baronti, S., 02
Benediktsson, Jon Atli, 0J
Bernat, Katarzyna, 1D, 1I
Bovolo, Francesca, 10
Bratsolis, E., 0Q
Brito, Victor, 07
Bruzzone, Lorenzo, 09, 10, 12
Bulatov, Dimitri, 0T
Camps Valls, G., 11
Carlà, R., 02
Castelletti, Davide, 12
Chan, Brigitte, 1P
Charou, E., 0Q
Chehdi, Kacem, 0H
Chen, Dong, 1M
Chen, Xiao, 1M
Chen, Zengping, 00, 17, 18, 1T
Cifarelli, Giuseppe, 0C
Corsini, Giovanni, 0X
D'Addabbo, Annarita, 1A
D'Addario, Larry, xi
Dal Poz, A. P., 0A
da Silva Pinho, Marcelo, 1V
De Ceglie, Sergio Ugo, 0Z
Dechoz, Cécile, 0B
Decker, Ryan K., xi
Delgado-Hernández, J., 14
Demir, Begüm, 12
Demirkesen, C., 0U
Deng, Xing Pu, 1E
Despini, Francesca, 03
Diani, Marco, 0X, 0Z
DiFilippo, David D. J., 1P
Diskin, Yakov, 0V
Domenech-Tofiño, E., 14
Drzewiecki, Wojciech, 1D, 1I
Duro, Nuno, 20
Eremeev, V., 0F
Fazan, Antonio J., 0A
Figueiredo, Isabel, 20
Gachet, Roland, 0B
Garzelli, A., 02
Gaudio, P., 13
Geldzahler, Barry, xi
Gelfusa, M., 13
Ghamisi, Pedram, 0J
Gómez-Chova, L., 11
Gonçalves, Gil, 20
Gong, Ting, 0I
Guccione, Pietro, 0C
Guo, Feng, 1Q
Guo, Jing, 1E
Guo, Shaofeng, 1K
Guo, Tao, 04
Gutiérrez, Rebeca, 0D
Gyftakis, S., 0Q
Han, Jian-tao, 0I
Hara, Konomi, 0P
Herumurti, Darlis, 0S
Hong, Yaohui, 1Q
Huddleston, Lisa L., xi
İdikut, Firat, 1N
Isola, Claudia, 0B
Ito, Leandro Hideyoshi, 1V
Jenssen, Robert, 0K
Jiang, Wanshou, 1C
Jiang, Yongmei, 1L
Jubelin, Guillaume, 15
Just, Dieter, 0D
Khenchaf, Ali, 15
Koutaki, Gou, 0S
Krupiński, Michał, 1D
Kuang, Gangyao, 1L
Kurt, Burak, 1X
Kuznetsov, A., 0F
Languille, Florie, 0B
Larsen, Siri Ø., 0K
Leloglu, Ugur M., 0U
Li, An, 1K
Li, Ji-cheng, 0I, 1M, 1U
Li, Jun, 1E

Li, Na, 00, 17, 18
 Li, Shanshan, 1K
 Liu, Fang, 17, 18, 1T
 Liu, Songlin, 00, 17, 1T
 Liu, Wen, 0P
 Liu, Yang, 17
 Liu, Yangyang, 21
 Lukin, Vladimir V., 0H
 Lv, Qunbo, 21
 Makarau, Aliaksei, 22
 Malizia, A., 13
 Manalo-Smith, Natividad, 1O
 Martimort, Philippe, 0B
 Mascolo, Luigi, 0C
 Massera, Stephane, 0B
 Mattar, Karim E., 19
 Matteoli, Stefania, 0X
 Michaelsen, Eckart, 1S
 Miller, Michael J., xi
 Min, Huang, 21
 Morabito, David D., xi
 Morgan, Jennifer G., xi
 Müller, Rupert, 22
 Muñoz-Marí, J., 11
 Murari, A., 13
 Myatov, G., 0F
 Niu, Zhaodong, 0O, 1T
 Nosavan, Julien, 0B
 Özkan, Vedat Ali, 1N
 Parracino, S., 13
 Pasquariello, Guido, 1A
 Peces Morera, J., 14
 Pelaes, Evaldo G., 07
 Petrucci, Beatrice, 0B
 Pinar, Sedef Kent, 1X
 Pinto, Luís, 20
 Pohl, Melanie, 0T
 Poshekhonov, V., 0F
 Presnyakov, O., 0F
 Priestley, Kory, 1O
 Pyka, Krystian, 1D
 Refice, Alberto, 1A
 Reinartz, Peter, 22
 Richetta, M., 13
 Richter, Rudolf, 22
 Rodríguez-Cuenca, B., 14
 Roeder, William P., xi
 Rossi, Alessandro, 0Z
 Rottensteiner, Franz, 0T
 Sabry, Ramin, 19
 Şahin, Asaf Behzat, 1N
 Salberg, Arnt B., 0K
 Santurri, L., 02
 Seibert, Marc A., xi
 Sévigny, Pascale, 1P
 Shi, Zhiguang, 1M
 Sidike, Paheding, 06, 0V
 Siravenha, Ana C., 07
 Smith, G. Louis, 1O
 Solano Correa, Yady Tatiana, 10
 Sousa, Erécilia, 20
 Svetelkin, P., 0F
 Takan, Taylan, 1N
 Tang, Min, 16
 Teggi, Sergio, 03
 Tragni, Mario, 0C
 Tremas, Thierry, 0B
 Tsenoglou, T., 0Q
 Tu, Ruibin, 0O
 Uchimura, Keiichi, 0S
 Uemura, Takumi, 0S
 Valcárcel Sanz, N., 14
 Varney, Nina M., 08
 Vassilas, N., 0Q
 Vega, J., 13
 Vozel, Benoit, 0H
 Wang, Pu, 1E
 Wang, Zhenhui, 16
 Wawrzaszek, Anna, 1D
 Wen, Gongjian, 1F
 Wu, Jian, 1L
 Xu, Xiaojian, 1Q
 Yamazaki, Fumio, 0P
 Yang, Lu, 16
 Yang, Wei-ping, 0I, 1U
 Yıldırım, İhsan Ozan, 1N
 Yue, Chunyu, 1C
 Zanetti, Massimo, 09
 Zemliachenko, Alexander N., 0H
 Zhan, Yizhe, 16
 Zhang, Jiangwei, 1T
 Zhang, Qing, 16
 Zhang, Xing, 1F
 Zhang, Yan, 0I, 1U
 Zhang, Yifan, 05
 Zhang, Zhilong, 1U
 Zhao, Hang, 16
 Ziems, Marcel, 0T

Conference Committee

Symposium Chair

Charles R. Bostater, Florida Institute of Technology (United States)

Symposium Co-chairs

Ulrich Michel, University of Education Heidelberg (Germany)

Bart Snijders, TNO (Netherlands)

Conference Chair

Lorenzo Bruzzone, Università degli Studi di Trento (Italy)

Conference Co-chairs

Jon Atli Benediktsson, University of Iceland (Iceland)

Francesca Bovolo, Fondazione Bruno Kessler (Italy)

Conference Programme Committee

Selim Aksoy, Bilkent University (Turkey)

Luciano Alparone, Università degli Studi di Firenze (Italy)

José M. Bioucas-Dias, Universidade Técnica de Lisboa (Portugal)

Gustavo Camps-Valls, Universidad de València (Spain)

Jocelyn Chanussot, Laboratoire des Images et des Signaux (France)

Chi-Hau Chen, University of Massachusetts Dartmouth (United States)

Melba M. Crawford, Purdue University (United States)

Fabio Dell'Acqua, Università degli Studi di Pavia (Italy)

Begüm Demir, Università degli Studi di Trento (Italy)

Peijun Du, Nanjing University (China)

Giles M. Foody, The University of Nottingham (United Kingdom)

Andrea Garzelli, Università degli Studi di Siena (Italy)

Jordi Inglada, Centre d'Etudes Spatiales de la Biosphère (France)

Gabriele Moser, Università degli Studi di Genova (Italy)

Allan A. Nielsen, Technical University of Denmark (Denmark)

Ryuei Nishii, Kyushu University (Japan)

Antonio J. Plaza, Universidad de Extremadura (Spain)

John A. Richards, The Australian National University (Australia)

Josiane B. Zerubia, INRIA Sophia Antipolis - Méditerranée (France)

Session Chairs

- 1 VHR Image Analysis and Fusion
Lorenzo Bruzzone, Università degli Studi di Trento (Italy)
- 2 Image Segmentation
Andrea Garzelli, Università degli Studi di Siena (Italy)
- 3 Geometric Corrections and Co-registration
Lorenzo Bruzzone, Università degli Studi di Trento (Italy)
- 4 Calibration, Restoration, and Compression
Lorenzo Bruzzone, Università degli Studi di Trento (Italy)
- 5 Feature Selection and Classification
Lorenzo Bruzzone, Università degli Studi di Trento (Italy)
- 6 Classification and Analysis of Urban Areas
Begüm Demir, Università degli Studi di Trento (Italy)
- 7 Analysis of Hyperspectral Data
Nicola Acito, Università di Pisa (Italy)
- 8 Change Detection and Analysis of Multitemporal Images
Francesca Bovolo, Fondazione Bruno Kessler (Italy)
- 9 Estimation and Detection
Luis Gómez-Chova, Universidad de València (Spain)
- JS1 SAR Data Analysis I: Joint Session
Lorenzo Bruzzone, Università degli Studi di Trento (Italy)
- JS2 SAR Data Analysis II: Joint Session
Claudia Notarnicola, EURAC research (Italy)

Remote sensing at the NASA Kennedy Space Center and the Eastern Range: a perspective from the ground up

Lisa L. Huddleston^{a*}, William P. Roeder^b,
David D. Morabito^c, Larry D'Addario^c, Jennifer G. Morgan^a,
Robert E. Barbré, Jr.^d, Ryan K. Decker^e,
Barry Geldzahler^f, Marc A. Seibert^a, Michael J. Miller^a

^aNational Aeronautics and Space Administration, Kennedy Space Center, FL,

^bUnited States Air Force, Patrick Air Force Base, FL,

^cNational Aeronautics and Space Administration, Jet Propulsion Laboratory, California Institute of Technology

^dNational Aeronautics and Space Administration, Marshall Space Flight Center, Jacobs

^eNational Aeronautics and Space Administration, Marshall Space Flight Center, AL

^fNational Aeronautics and Space Administration, Headquarters, DC

ABSTRACT

This paper provides an overview of ground based operational remote sensing activities that enable a broad range of missions at the Eastern Range (ER), which includes the National Aeronautics and Space Administration (NASA) Kennedy Space Center (KSC) and U.S. Air Force Cape Canaveral Air Force Station (CCAFS).

Many types of sensors are in use by KSC and across the ER. We examine remote sensors for winds, lightning and electric fields, precipitation and storm hazards. These sensors provide data that are used in real-time to evaluate launch commit criteria during space launches, major ground processing operations in preparation for space launches, issuing weather warnings/watches/advisories to protect over 25,000 people and facilities worth over \$20 billion, and routine weather forecasts. The data from these sensors are archived to focus NASA launch vehicle design studies, to develop forecast techniques, and for incident investigation. The wind sensors include the 50-MHz and 915-MHz Doppler Radar Wind Profilers (DRWP) and the Doppler capability of the weather surveillance radars. The atmospheric electricity sensors include lightning aloft detectors, cloud-to-ground lightning detectors, and surface electric field mills. The precipitation and storm hazards sensors include weather surveillance radars.

Next, we discuss a new type of remote sensor that may lead to better tracking of near-Earth asteroids versus current capabilities. The Ka Band Objects Observation and Monitoring (KaBOOM) is a phased array of three 12 meter (m) antennas being built as a technology demonstration for a future radar system that could be used to track deep-space objects such as asteroids. Transmissions in the Ka band allow for wider bandwidth than at lower frequencies, but the signals are also far more susceptible to de-correlation from turbulence in the troposphere, as well as attenuation due to water vapor, which is plentiful in the Central Florida atmosphere. If successful, KaBOOM will have served as the pathfinder for a larger and more capable instrument that will enable tracking 15 m asteroids up to 72 million kilometers (km) away, about half the distance to the Sun and five times further than we can track today.

Finally, we explore the use of Site Test Interferometers (STI) as atmospheric sensors. The STI antennas continually observe signals emitted by geostationary satellites and produce measurements of the phase difference between the received signals. STIs are usually located near existing or candidate antenna array sites to statistically characterize atmospheric phase delay fluctuation effects for the site. An STI measures the fluctuations in the difference of atmospheric delay from an extraterrestrial source to two or more points on the Earth. There is a three-element STI located at the KaBOOM site at KSC.

* Corresponding author: lisa.l.huddleston@nasa.gov; phone 1 321 861-4952; fax 1 321 861-7907

Keywords: Remote sensing, Eastern Range (ER), Kennedy Space Center (KSC), Cape Canaveral Air Force Station (CCAFS) weather, radar, lightning sensors, Doppler Radar Wind Profilers (DRWPs), antenna arrays, atmospheric fluctuations, coherent uplink, phased arrays, adaptive optics, site test interferometers (STIs)

1. INTRODUCTION

Remote sensing has become a common term in atmospheric and environmental discussions. The vast majority of the references deal with data produced by space based or "satellite remote sensing" instruments. There is however a broad range of remote sensing applications that are ground based. A number of these applications are currently in use at the Eastern Range (ER, Appendix A contains an acronym list) which includes Kennedy Space Center (KSC) and Cape Canaveral Air Force Station (CCAFS) in Florida (FL) to support a broad range of National Aeronautics and Space Administration (NASA), United States Air Force (USAF) and commercial space launch missions. This paper describes the vital role that ground based remote sensing plays in launch operations, personnel safety, resource protection, and historical databases for mission planning and forecast improvement; in deep space investigations; and in research to measure the effects of turbulence in the atmosphere on space communication, navigation and radar signals.

2. WEATHER AND LAUNCH OPERATIONS

Comprehensive weather services to the United States of America's space program at the ER is provided by the USAF's 45th Weather Squadron (45WS)¹. To provide these services, the ER and 45WS use extensive networks of ground-based instrumentation to ensure successful launch operations and to aid in vehicle design. These networks comprise the most unique and dense suite of weather sensors found in operational meteorology today. Lightning detection systems, specifically the Launch Pad Lightning Warning System (LPLWS), the Four Dimensional Lightning Surveillance System (4DLSS), and the National Lightning Detection Network (NLDN), are used to detect lightning and assess the Lightning Launch Commit Criteria (LCC). The C-Band Weather Radar assists in applications that include high precision lightning forecasting, evaluating lightning LCC, stringent convective wind prediction, severe weather warnings, hail detection, heavy rain advisories, and warning of local tropical system threats. The Doppler Radar Wind Profiler (DRWP) system provides wind profiles used to evaluate loads on both day-of-launch and during vehicle design assessments.

Weather is the leading cause for launch scrubs and delays and has a large impact on many aspects of space launch activities. These include active launch operations, ground processing operations in preparation for launch, post-launch operations, various special missions, routine 24/7 weather watch and warning responsibilities for personnel safety, resource protection and mission planning. During launch countdowns, the 45WS forecasts and evaluates the Lightning LCC, Range LCC, and User LCC². [2] The Lightning LCC are a set of complex rules used to avoid natural and rocket triggered lightning^{3,4,5}. The Range LCC include boundary layer profiles of wind, temperature and moisture that are primarily used for predicting transport and dispersion of atmospheric constituents. This is especially important in the event of an explosion or other major malfunction where toxic chemicals are released into the atmosphere. Many atmospheric phenomena generate and/or store electrical charge that is insufficient to cause natural lightning. However, when a large rocket flies near those areas of electric charge, the long conductive exhaust plume and length of the metal rocket can amplify the associated electric fields by a factor of over 100. If the amplified electric field exceeds the breakdown voltage of the air, a rocket triggered lightning occurs. While the lightning can damage the rocket itself, or more likely the onboard electronics, the greatest concern is the lightning may damage the flight termination system. This would stop the ability of the flight controllers from being able to destroy the rocket if it goes too far off course. The User LCC are limits for various weather categories such as near surface winds so the rocket can safely clear the launch tower, temperature for mechanical integrity of the rocket, and precipitation to avoid damaging the rocket while in-flight. Requirements also exist for upper level winds to avoid over stressing the space launch vehicle as it counter-steers through the actual winds versus the planned winds to stay on the correct trajectory and achieve the desired orbit. The User LCC varies between launch vehicle programs and different configurations of vehicles in the same program⁶.

The 45WS is responsible for the weather safety of over 25,000 personnel and resource protection for over \$20 billion of facilities, not including the payloads and space launch vehicles. Each year, the remote sensing capabilities at KSC facilitate the issuance of over 2,500 weather warnings, watches, and advisories. These include warnings for tornadoes, large hail, strong winds, and imminent or occurring lightning; watches for convective winds, steady state winds, developing lightning, and heavy rain; and advisories for temperature. Over 5,000 ground processing operations are

performed annually in preparation for space launches⁷. Major ground processing operations include vehicle rollouts to the launch pads, stacking and destacking rocket segments, transporting and mounting and demounting payloads, and large crane operations. Crane lifts can be very wind sensitive, especially when lifting fueled solid rocket boosters, multi-billion dollar payloads, or multi-million dollar rocket segments. Minor operations can be as simple as performing corrosion maintenance on the launch pads. Many of these processing operations are conducted outside and must be curtailed under certain weather conditions. Some processing operations have restrictive weather limits that can result in weeks of delay⁶.

The hazards of lightning, both natural and triggered, are well known and include direct and indirect effects. Direct effects include heating, pitting or melt-through of conducting materials, puncturing or splintering of nonmetallic surfaces, burning holes in the skin, the welding or fusing of hinges and bearings; damage to antennas and/or lights; and, rarely, explosions due to the ignition of fuel vapors⁸. Indirect effects include any momentary upsets or permanent damage caused by the transient voltages and currents that are induced by direct or nearby discharges⁸. For most spacecraft, the penalties in added cost and weight of hardening against these hazards are too great, so the only option is avoidance⁹. Lightning is also a significant weather safety hazard, being the third leading source of storm deaths in the United States¹⁰. [10] Lightning advisories are issued for 10 areas, consisting of circles with a 9.26 kilometer (km, 5 nautical mile (NM)) or 11.11 km (6 NM) radii safety buffer centered on operationally significant sites: seven areas with considerable overlap on CCAFS/KSC, one with little overlap on KSC, one at Patrick Air Force Base (AFB), and one for a satellite processing facility at Titusville (Figure 1). A Phase-I Lightning Watch is issued for one or more of these areas if lightning is expected with a desired lead-time of 30 min. A Phase-II Lightning Warning is issued when lightning is imminent or occurring in one or more of these areas. One of the greatest challenges is the ability to reliably cancel these lightning advisories more quickly to allow outdoor work to resume, while still maintaining safety⁶. As one might expect with all the thunderstorm activity, convective wind warnings are also important, with an average of over 175 warnings each year. The convective wind warnings have unusually precise requirements and large desired lead-times⁶.

In addition to those items already discussed, four other aspects of launch are evaluated for weather concerns. The first launch aspect is 'LOADS', which refers to the aerodynamic loading on the rocket as it counter-steers against the upper-level winds to stay on the desired trajectory. If the actual winds differ too much from the assessed winds, the rocket could destroy itself. The LOADS community of aeronautical engineers continually analyzes the observed winds and assesses their impact to the vehicle to prevent this from happening. There is an extensive archive of vertically complete wind profiles generated by the Marshall Space Flight Center (MSFC) Natural Environments (NE) group using the DRWP network at the ER. This archive is used to mitigate the multiple shortcomings of utilizing balloon-based measurements for space vehicle loads and trajectory assessments. Launching vehicles into space requires accurately characterizing the wind environment that the vehicle will experience through ascent. Specific effects of the ascent winds on launch vehicles depend on the characteristics of the vehicle components and the magnitude of the wind acting on those components¹¹. Range Safety evaluates the second, third, and fourth aspects of launch: 'Toxic Dispersion', 'BLAST', and 'Debris'¹². Toxic dispersion from nominal and catastrophic launches is analyzed to ensure that they will not exceed allowable toxic exposure limits for the on-base and nearby civilian populations. 'BLAST' analyzes the likelihood of windows in nearby towns being broken and causing a safety hazard if a rocket explodes¹³. The 'Debris' program considers if parts of the rocket from a nominal or catastrophic launch would fall outside of the allowed impact areas⁶.

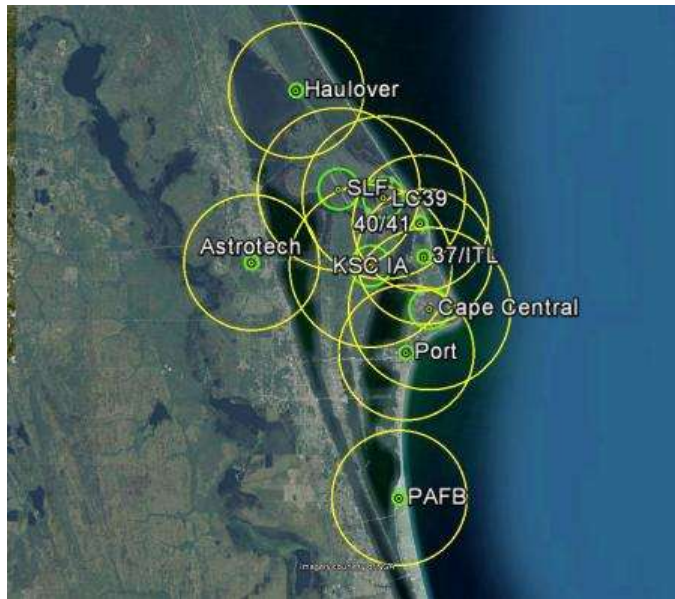


Figure 1. The 10 lightning warning circles used by 45 WS.

2.1 Eastern Range Weather Systems

The ER possesses one of the world’s most dense operational networks of weather instrumentation¹⁴. This instrumentation is used to minimize the impact of weather while ensuring the safe processing and launching of space vehicles. Some, but not all, of these weather instruments use remote sensing. For example, the ER uses a network of 28 weather towers that measures wind, temperature, and moisture in the first few hundred feet of the atmosphere. However, this paper will focus only on the ER weather instruments that use ground-based remote sensing. These include lightning detection systems, the DRWPs, and the weather radar. The ground-based remote sensing weather sensors and the data they provide are listed in Table 1.

Table 1. Ground-based remote sensing weather sensors at the Eastern Range

Sensor	Data Provided	Main Operational Applications
Four Dimensional Lightning Surveillance System (4DLSS)	<ul style="list-style-type: none"> • Cloud-to-Ground Lightning <ul style="list-style-type: none"> - return strokes (not flashes) - latitude, longitude - date, time - peak current, polarity • Lightning aloft <ul style="list-style-type: none"> - step leaders - latitude, longitude, height - date, time 	<ul style="list-style-type: none"> • Assess risk of induced current damage, Lightning warnings (approaching storms), Evaluate Lightning LCC • Lightning warnings Evaluate Lightning LCC
Launch Pad Lightning Warning System (LPLWS)	<ul style="list-style-type: none"> • Surface electric field 	<ul style="list-style-type: none"> • Evaluate Lightning LCC
Weather Radar	<ul style="list-style-type: none"> • Reflectivity • Doppler velocity • Spectral width • Differential reflectivity 	<ul style="list-style-type: none"> • Lightning prediction, Lightning LCC evaluation, severe weather warnings, precipitation detection, general weather support • Severe weather warnings • None • Possibly lightning onset and hydrometeor identification for lightning cessation, hail

Sensor	Data Provided	Main Operational Applications
	<ul style="list-style-type: none"> • Phase differential • Correlation coefficient 	warnings, tornado detection, etc. <ul style="list-style-type: none"> • Possibly hydrometeor identification for lightning cessation, hail, tornado, etc. • Possibly hydrometeor identification for lightning cessation, hail, tornado, etc.
50-MHz Doppler Radar Wind Profiler (50DRWP)	<ul style="list-style-type: none"> • Vertical wind profiles <ul style="list-style-type: none"> - wind speed/direction vs. height (base-top) 	<ul style="list-style-type: none"> • Evaluate LOADS
915-MHz Doppler Radar Wind Profiler (915DRWP)	<ul style="list-style-type: none"> • Vertical wind profiles <ul style="list-style-type: none"> - wind speed/direction vs. height (base-top) 	<ul style="list-style-type: none"> • Evaluate toxic dispersion, BLAST, and Debris

2.2 Lightning Detection Systems

The ER is well instrumented with respect to lightning detection sensors. These sensors exist not only because lightning can adversely affect the vehicle and corresponding operations, but also because central Florida is the area of highest lightning activity in the United States (U.S.)¹⁵ The ER utilizes the Launch Pad Lightning Warning System (LPLWS), the Four Dimensional Lightning Surveillance System (4DLSS), and the National Lightning Detection Network (NLDN) to detect lightning.

The LPLWS consists of a network of 31 field mills distributed in and around the launch and operations areas of CCAFS and KSC. The location of the 31 mills is shown in Figure 2 and picture of one of the field mills is shown in Figure 3 The network measures the electric field at the surface, which is used to infer electric fields aloft - a key to evaluating the danger of triggered lightning during launch operations¹⁴. In the Lightning LCC, field mills can be used to either avoid launch under hazardous conditions, or to allow safe launch that otherwise would have been falsely identified as hazardous. The one-minute average of the electric field mill network may not exceed -1 or +1 kilovolts per meter (kV/m) within 9.26 km (5 NM) of the launch pad or the lightning flash at any time within 15 minutes prior to launch. This field mill criteria becomes -1.5 or +1.5 kV/m if there are no clouds within 18.52 km (10 NM) of the flight path except those that are transparent^{3,4,5}.

The 4DLSS detects both cloud-to-ground return strokes and lightning aloft^{16,17}. [16] The 4DLSS was a major upgrade to the previous Lightning Detection and Ranging (LDAR) system that detected lightning aloft and the Cloud to Ground Lightning Surveillance System (CGLSS)^{16,17}. The cloud-to-ground lightning part of the network consists of a network of six low frequency (LF) magnetic direction-finding and time-of-arrival (IMPACT) sensors located in and around the launch and operations areas of CCAFS and KSC (Figure 4). A picture of one of these sensors is shown in Figure 5. They are deployed on relatively short baselines and operate at low gain to ensure the requirements for high location accuracy and detection efficiency of cloud-to-ground strikes are satisfied¹⁴. This part of 4DLSS provides the latitude, longitude, time, peak current, and polarity for each return stroke within a lightning flash. The lightning aloft part of 4DLSS consists of a network of nine receiver sites which detect inter-cloud, intra-cloud and cloud-to-ground lightning. Lightning aloft is geolocated using VHF time-of-arrival between multiple pairs of sensors¹⁴. The locations of the sensors is shown in Figure 6 with an example of one of the sensors is at Figure 7. The time-of-arrival differences between multiple pairs of sensors is used to locate the three dimensional (3-D) structure of the lightning. The 4DLSS is being replaced with a new system to overcome sustainment problems of the old sensors and take advantage of improvements in lightning detection technology. The new system is the Mesoscale Eastern Range Lightning Network (MERLIN).

The 45WS also has a direct link to the NLDN, which is a network of about 130 cloud-to-ground sensors across the contiguous U.S.¹⁸ The NLDN is also has a relatively new low detection efficiency capability for detecting lightning aloft. This NLDN link is used as a back-up to the cloud-to-ground portion of 4DLSS, for cloud-to-ground lightning detection capability for occasional missions beyond the range of 4DLSS, and as supplemental quality control of 4DLSS cloud-to-ground lightning.

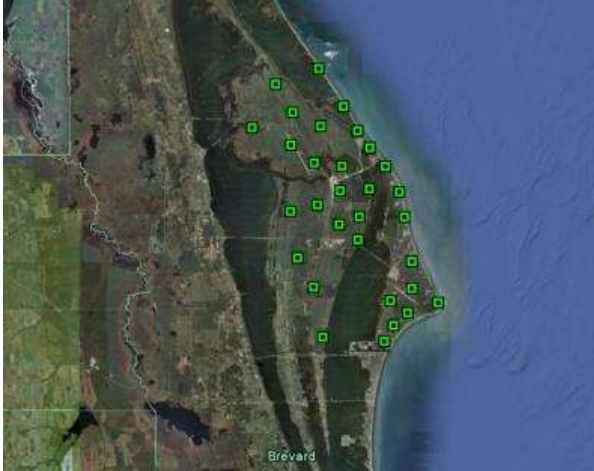


Figure 2. Field mill sensor locations.



Figure 3. A field mill sensor.

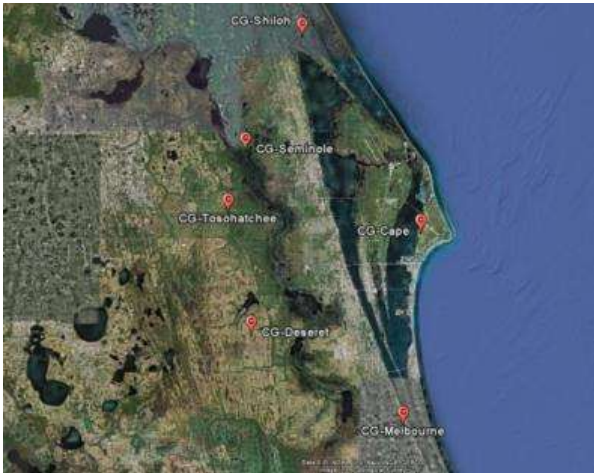


Figure 4. CGLSS sensor locations.



Figure 5. A CGLSS sensor.

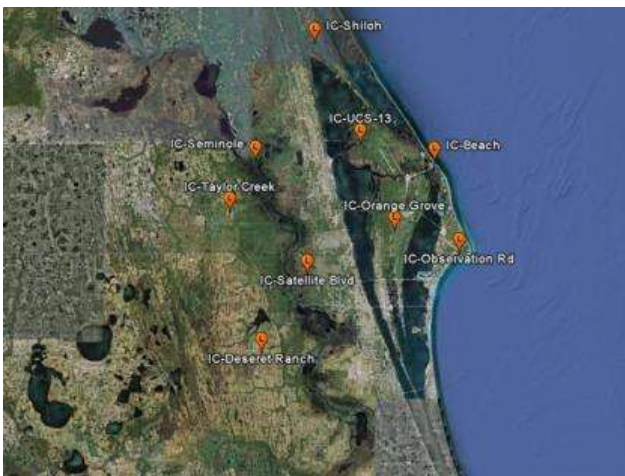


Figure 6. An LDAR-II sensor.



Figure 7. LDAR-II sensor locations.

2.3 Weather Radar

One of the most important weather sensors is the C-band (5 cm) Radtec Titan Doppler Radar with 4.3 m diameter antenna and 250 kW average transmitted power (TDR 43-250) manufactured by Radtec Engineering, Inc¹⁹. The space program on the ER makes use of several atypical applications of weather radar²⁰. These applications include high precision lightning forecasting, evaluating lightning LCC, stringent convective wind prediction, severe weather warnings, hail detection, heavy rain advisories, and warning of local tropical system threats²⁰. The location of the 45WS radar and a picture of the radar are shown in Figure 8 and

Figure 9, respectively.

The TDR 43-250 radar is a dual polarization Doppler weather surveillance radar that detects reflectivity, Doppler velocity, spectral width, differential reflectivity, phase differential, and correlation coefficient. Reflectivity indicates the intensity of precipitation, and the shape and motion of thunderstorms that can imply the type and intensity of hazard they may produce. Reflectivity is especially useful in forecasting the onset of lightning in locally developing thunderstorms^{21,22} and in evaluating Lightning LCC. Doppler velocity can detect storm rotation that can indicate severe weather, especially tornadoes. Differential reflectivity, phase differential, and correlation are new dual polarization capabilities that should have many new capabilities including lightning formation^{21,22}, lightning cessation, hail detection, tornado detection²³, and eventually Lightning LCC evaluation.

The 45WS also has a direct feed from the Weather Surveillance Radar – 1988 Doppler (WSR-88D radar) at Melbourne, FL. This radar is part of the Next Generation Weather Radar (NEXRAD) network shared by the Department of Defense (DoD), National Weather Service (NWS), and the Federal Aviation Administration (FAA). This radar is an S-band (10 cm) dual polarization Doppler weather surveillance radar. This radar serves as a back-up to the Radtec radar and provides dual wavelength capability in combination with the 45WS radar.

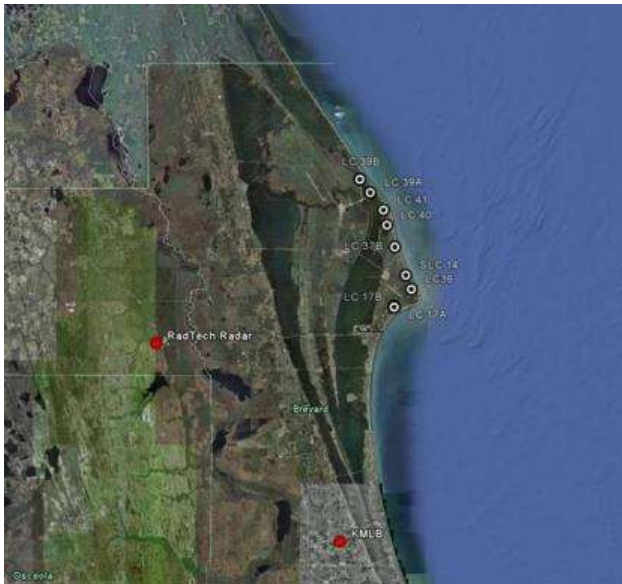


Figure 8. Locations of radars used by 45WS.



Figure 9. 45WS C-band weather radar.

2.4 Doppler Radar Wind Profilers

A Doppler Radar Wind Profiler (DRWP) is a radar system designed to detect the Doppler shift of clear-air turbulence in order to measure vertical profiles of wind. DRWPs work by transmitting radio pulses along two or more beams and using the Doppler shift of the returned signals from the two vectors to calculate the wind vector, and use different frequencies and different transmission powers depending on maximum height of wind required. DRWP systems are remote sensors and the maximum height probed varies with atmospheric conditions and especially latitude²⁴. The MSFC NE group generates an extensive archive of vertically complete wind profiles using the DRWP network at the ER to

mitigate the shortcomings of utilizing balloon-based measurements for space vehicle loads and trajectory assessments. Launching vehicles into space requires accurately characterizing the wind environment the vehicle will experience during ascent. Specific effects of the ascent winds on launch vehicles depend on the characteristics of the vehicle components and the magnitude of the wind acting on those components¹². The shortfall of balloon measurements of winds are long sensing time (over 1.5 hours to measure winds from surface to ~30,000 m), downwind drift of the balloon (up to 280 km downwind or more at ~30,000 m), and pendulum motion of the sensor at the end of the 30 m string attached to the balloon.

2.4.1 50-MHz DRWP

Every launch passes through the atmosphere. Winds below altitudes of 18 - 20 km (60 - 65 kft) are a major concern for safety and mission assurance, guidance and steering, and aerodynamic loads. The 50-MHz DRWP is located just east of the Shuttle Landing Facility at KSC (Figure 10). The former 50-MHz DRWP consisted of an irregular octagon-shaped antenna field, which spanned 15,600 square meters (m) and consisted of coaxial-collinear elements set 1.5 m above the ground plane made of copper wire. These elements sent electronic pulses at 49.25 MHz through three beams. One beam pointed vertically, and two oblique beams pointed 15° off zenith at azimuths of 45° and 135° East from due North (Figure 11). To measure wind velocities, the 50-MHz DRWP sent radio pulses in the three beam directions sequentially and measured the return signals that were reflected by temperature and humidity fluctuations in the atmosphere. Bragg Scattering designates this process, where changes in temperature and humidity with length scales of about half of the DRWP's wavelength, (~3 m for the 50-MHz DRWP), produce the return signal. A Fast Fourier Transform converted the signal in the time-domain to the frequency domain (Doppler power spectra) over 256 frequency bins at each range gate. There were 111 range gates from 2,666-18,616 m every 145 m and profiles were generated every three minutes¹².

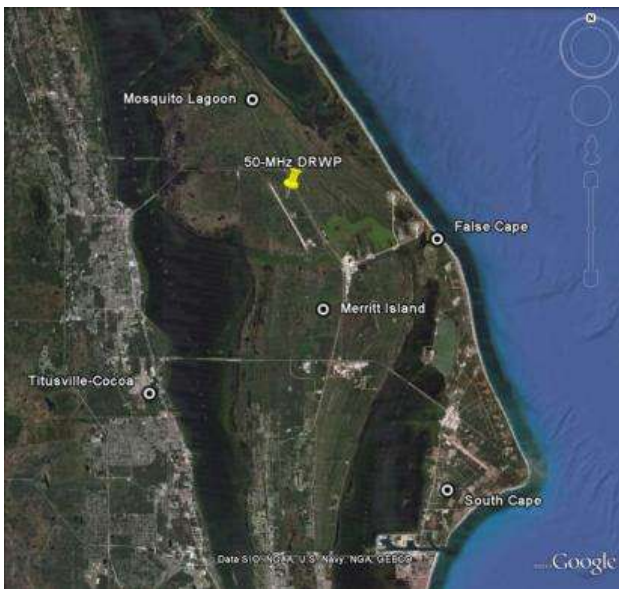


Figure 10. 50-MHz DRWP location at the ER.

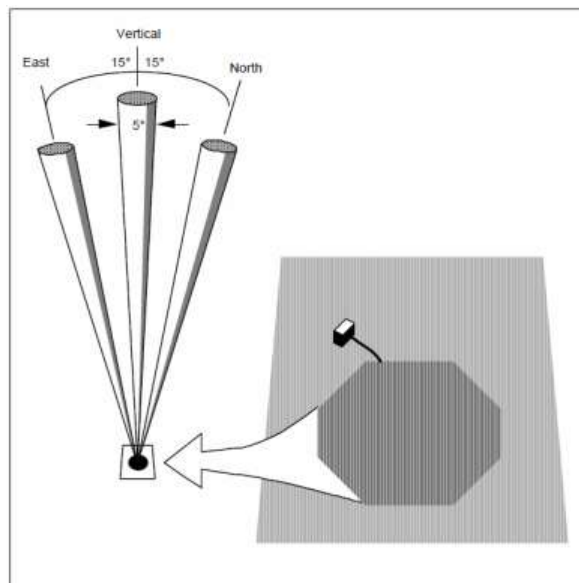


Figure 11. A schematic of the DRWP's beam configuration¹².

Currently this system is being replaced by a new 50-MHz DRWP manufactured by DeTect, Inc. The antenna of the new system will have a full beam steering (FBS) capability. (NASA will use specific pointing directions, however.) It is of a scalable design and is primarily soft-fail. The new antenna is comprised of 640 Yagi elements arranged in a thinned pattern. Each Yagi element transmits at the same power level and the antenna amplitude taper minimizes sidelobes.

This new 50-MHz DRWP, which is based on the NOAA National Profiler Network²⁴ contains a solid state 250 kW transmitter, solid state programmable phase switching, and permits additional operating modes such as 4-beam and Velocity Azimuth Display (VAD) modes without modification.

2.4.2 915-MHz Boundary Layer DRWP Network

A network of five 915-MHz DRWPs is arranged in a diamond-shaped pattern around the periphery of the ER (Figure 12). The 915-MHz DRWP is smaller than the 50-MHz DRWP due to its antenna structure, and thus one can use more of them in a given region. Figure 13 shows a picture of one of the 915-MHz DRWPs in the region. The network's configuration allows for each 915-MHz DRWP to potentially sample a different atmospheric boundary layer regime, especially in a dynamic environment¹². This network was installed to fill the gap from the top of the wind towers to the lowest gate of the 50-MHz DRWP. Vertical profiles are generated from 120-5,000 m every 100 m and profiles are generated every fourteen minutes. The system's primary mission objectives are: (1) to collect wind profiles for use by the Launch Weather Officer to monitor rapidly changing weather conditions, help ensure that launch constraints are satisfied, and to provide Range Users with timely guidance during the countdown and launch pad operations; (2) to monitor rapidly changing weather conditions that could affect ground and launch operations by Range Safety and as an input to the Range Safety models used to predict the transport and diffusion of airborne contaminants released from ground level spills; and (3) to provide forecasters with a continuous description of the intermediate levels of the atmosphere for routine weather forecasting and the early detection of hazardous conditions²⁵.

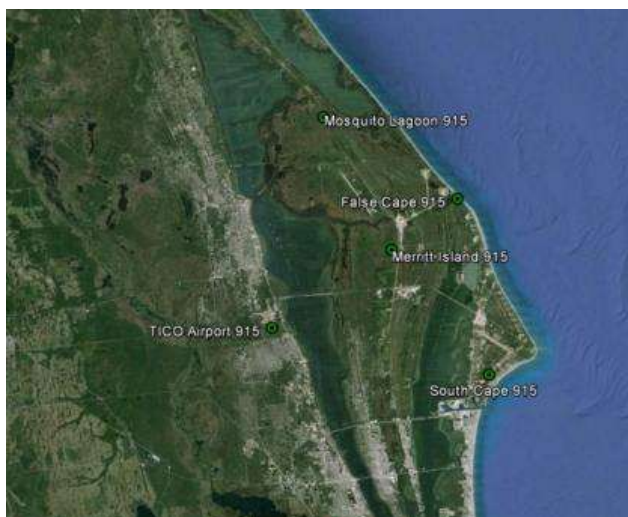


Figure 12. 915-MHz DRWP locations at the ER.



Figure 13. A 915-MHz DRWP at the ER.

3. KA BAND OBJECT OBSERVATION AND MONITORING

3.1 KaBOOM

The weather sensing technologies for processing and launching rockets will be of little use if a piece of orbital debris destroys a spacecraft in orbit or if a potentially hazardous asteroid or comet is on a collision course with the Earth. Therefore, NASA has embarked on a path to implement a high power, high resolution radar system to better track and characterize near-Earth objects (NEOs) and orbital debris. KaBOOM is a phased array of three 12 meter (m) diameter antennas at KSC. NASA is exploring the use of small diameter antennas as a phased radar array that is both scalable and extensible to achieve high power, high resolution, high reliability, simultaneous multiple direction operations, low life cycle cost, and elimination of power density restrictions. Applying this technique of coherent uplink arraying would produce a more reliable, available, scalable, extensible radar with a lower life cycle cost²⁶.

3.2 Potentially Hazardous Asteroids (PHA's)

If an object is verified to be on an Earth colliding trajectory, it seems likely that this collision possibility will be known several years prior to the actual event²⁷. With this lead time, existing technology could be used to mitigate the threat to the Earth. In the short term, the probability of an Earth impact is low, however, over longer periods of time, the probability of Earth impact is not negligible. One can view the probability of potential Earth impact events based on

currently available observations in the Jet Propulsion Laboratory (JPL) Near-Earth Object (NEO) Program Sentry Risk Table at <http://neo.jpl.nasa.gov/risk/>.

Potentially Hazardous Asteroids (PHAs) are defined based on the asteroid's potential to make threatening close approaches to the Earth. Specifically, all asteroids with an Earth Minimum Orbit Intersection Distance (MOID) of 0.05 AU (4,650,000 miles) or less, and asteroids smaller than about 150 m (500 ft) in diameter are not considered PHAs. There are currently 1487 known PHAs²⁷.

This "potential" to make close Earth approaches does not mean a PHA will impact the Earth. It only means there is a possibility for such a threat. By monitoring these PHAs using phased array antennas such as those being demonstrated by KaBOOM, and updating their orbits, we will be able to better predict the close-approach statistics and their Earth-impact threat²⁷.

Besides 24/7 availability for planetary protection (NEO tracking and characterization), NASA has several other uses for uplink arraying: improved detection and tracking of small ($\leq 1 - 10$ cm) orbital debris particles; rapidly available high power emergency uplink capability for spacecraft emergencies; radio science experiments (tomography of planetary atmospheres, general relativity tests, mass determinations, occultations, surface scattering, etc.); and beam sailing propulsion capability²⁶.

3.3 The Demonstration Project

The KaBOOM demonstration consists of a phased array of three 12 m diameter antennas, shown in Figure 14 below. It is intended to extend prior experiments to higher frequencies, and will eventually operate near 30 GHz. Its main features are the ability (a) to produce phase-aligned signals at a distant target without external calibration, and (b) to use a downlink signal (if one is simultaneously present) to measure the effects of tropospheric turbulence along the signal paths and apply real-time corrections to the uplink signal. The effects of tropospheric turbulence increase in proportion to signal frequency, as do the effects of errors in the instrumentation^{28,29}, making the KaBOOM demonstration particularly challenging.

In 2008, uplink arraying demonstrations were carried out by two different groups at JPL, one using two and three of the Goldstone Deep Space Network (DSN) site's 34 m at 7.2 GHz³⁰ and another using five 1.2 m antennas at 14 GHz³¹. Both demonstrations were successful. The systems were stable and the expected change in power at the target with number of active antennas was observed. (For identical antennas and transmitters, the received power for an N-antenna array is N^2 times that of one antenna.) There was no correction for atmospheric turbulence in either case.

In 2010, NASA funded an uplink array demonstration at 8 GHz using three 12 m antennas in Melbourne, FL. That experiment seemed to show that phase-aligned signals at the target can be achieved without external calibration by using internal phase-transfer electronics and correcting for measured mechanical differences among the antennas^{29,32}. Furthermore, it was demonstrated that real-time compensation for tropospheric turbulence may be possible when there is a strong reference source in the antenna beams, such as a beacon on the target satellite. The atmosphere compensation was demonstrated not only in clear, relatively dry air, but also during Tropical Depression 16/Tropical Storm Nicole (Figure 15)³². The present KaBOOM demonstration is using the very same 12 m antennas and some of the electronics that were used in the Melbourne experiment, although completely new electronics and more precise mechanical measurements will be needed at 30 GHz.



Figure 14. KaBOOM antennas at KSC.

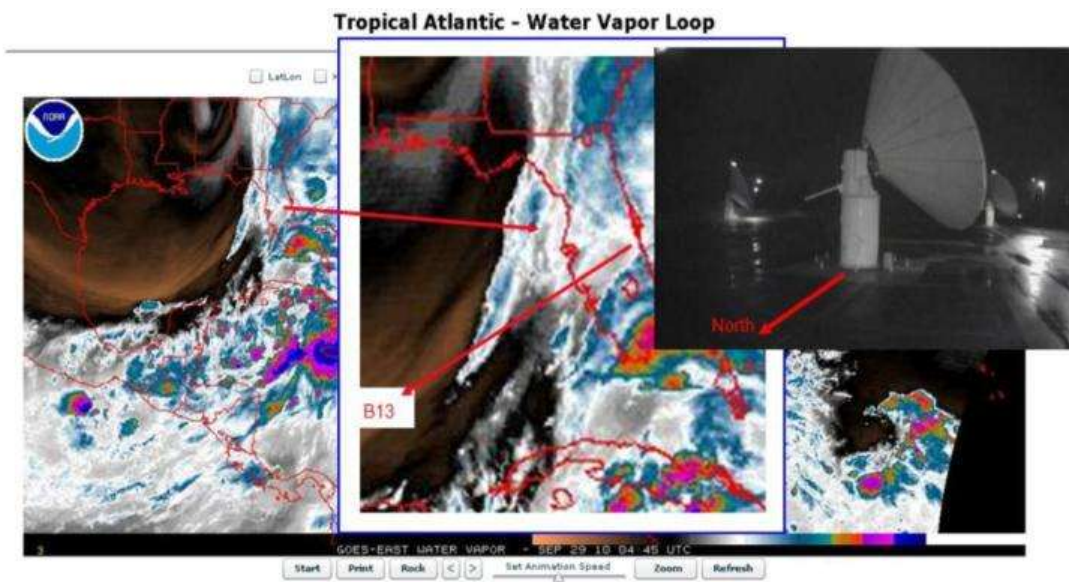


Figure 15. Tropical Atlantic water vapor loop showing environmental conditions during testing of the real-time atmospheric fluctuation compensation test in September 2010. Tropical Depression 16, September 29, 2010, 04:45 UTC. Light rain and substantial irregular water vapor content along pathway.

4. SITE TEST INTERFEROMETERS

4.1 Transition to Higher Frequencies

As NASA progresses into the 21st century, its communications network systems (e.g., Deep Space and Near Earth Networks) are expected to transition frequencies above 30 GHz. These systems will be required to provide services with a system availability of higher than 99% (versus the current 90% availability) and gigabit data rates (versus current ~ megabit data rates). However, the atmospheric phase stability (time delay fluctuations) and attenuation of a particular site must be well characterized.

A Site Test Interferometer (STI) measures the difference in signal delay from a celestial source (typically a geostationary satellite) to two or more points on the Earth. Variations in that delay difference are primarily due to turbulence in the troposphere, which creates a difference in the mean refractive indices along the paths³³.

An STI constructed by the JPL and based on a design provided by the Harvard Smithsonian Center for Astrophysics (CfA) has been installed at KSC. Nearly identical instruments have been deployed by JPL at five additional sites around the world, and other STIs have been in operation at radio observatories for many years. The KSC STI uses three small (0.8 m) antennas in a triangular configuration with spacings of 135 to 289 m to receive and process signals from a commercial geostationary satellite (NIMIQ 5, azimuth 163.8° and elevation 55.6°). The observed turbulence varies with weather and season, but its effect over ~200 m distance scales is not measurable by ordinary meteorological instruments, hence the need for a specialized instrument. While the STI is designed to provide a long-term statistical characterization of the site, it will also help KaBOOM to determine how much its signals are being disrupted by the atmosphere in near-real-time, and thus provide a measure of how well KaBOOM's atmosphere compensation process is working³⁴.

4.2 Operational Sites

Two STIs have been operating at the NASA DSN site in Goldstone, California for several years³³. These instruments have two and three antennas, respectively, with element separations of ~200 m. Three-element STIs have also been installed at the Canberra and Madrid DSN sites. The antennas continuously observe signals emitted by geostationary satellites, and the phase difference of the received signals is measured. During post-processing, long period trends due to satellite motion and instrumental drift are removed. Fluctuations in the resulting phase delay residuals are dominated by the troposphere on timescales ranging from <<1 s to several hundred seconds³³.

Although an STI and a nearby communication array or radio telescope are expected to see the same short- and long term statistical delay fluctuations, the instantaneous delay measured by the STI is generally not useful for correcting delay errors in the array because their targets are in different directions and their signals pass through different parts of the turbulent distribution. However, the statistics acquired over long periods are useful for characterizing the site.

The statistics vary among sites due to climate and altitude and at any one site diurnally, seasonally, and with passage of weather systems. The long-term statistics can be used to determine the suitability of a site for hosting an array, or they can be used in communication link budgets of current or proposed missions using an array at the site. Short-term (intraday) statistics can be used to assist in scheduling communication links so that the best conditions are used for links with small margins, and conversely³³.

We intend to operate the STI several years in order to obtain sufficient data for reliable statistical characterization of our KaBOOM site. The KaBOOM/STI location is shown in Figure 16 and a picture of one of the STI elements is shown in Figure 17. Figure 18 displays the zenith delay root mean square (RMS) for all three KSC STI baselines for the month of September 2013. One can clearly see a diurnal variation, where the delay RMS peaks within a few hours of local noon. Figure 19 displays the cumulative distribution of the delay RMS for several months since the instrument started operations in August 2013. One can clearly see a seasonal trend where the zenith delay RMS is higher during summer than during the winter for a given CD value.

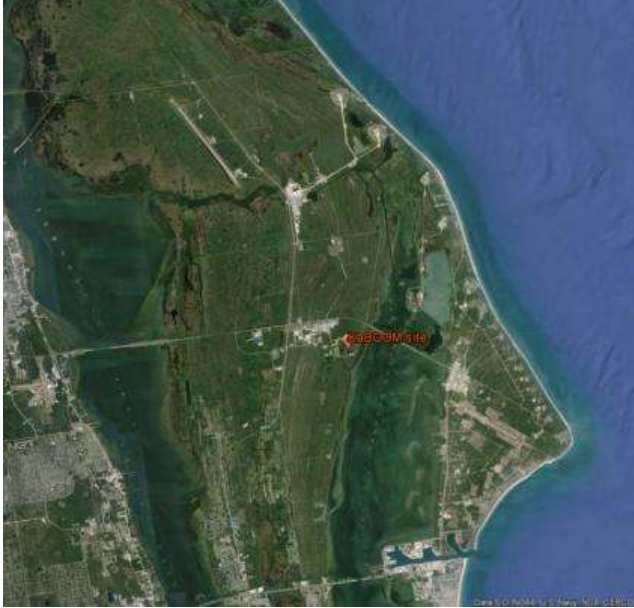


Figure 16. Location of the KaBOOM antennas and STI instrument at KSC.

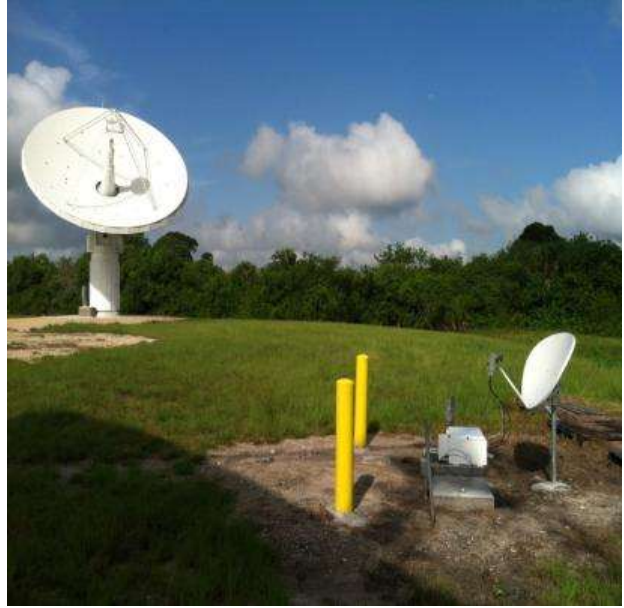


Figure 17. Foreground: one of three small antennas that make up the STI instrument. Background: one of the larger antennas of the KaBOOM demonstration.

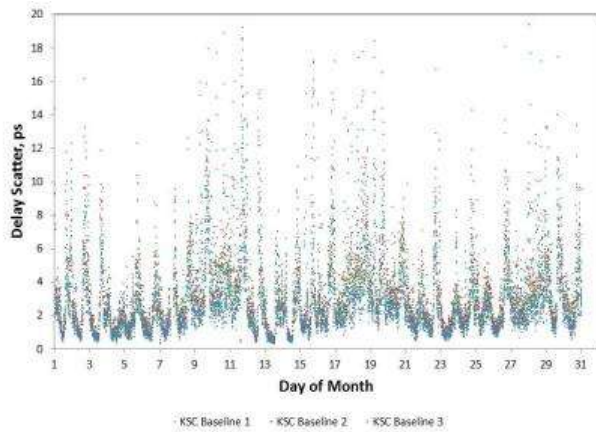


Figure 18. Delay RMS in 600-s blocks referenced to zenith for the KSC STI (all three baselines).

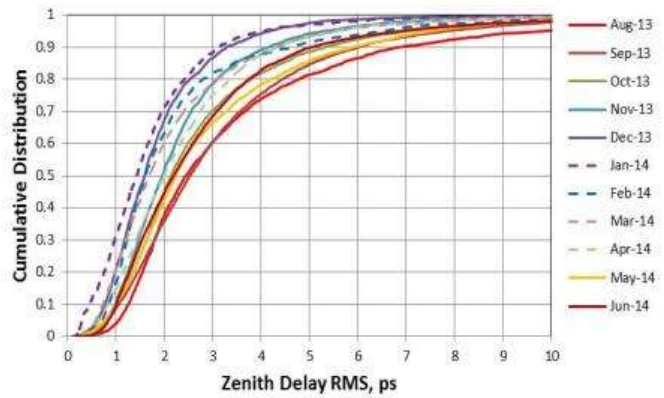


Figure 19. Monthly cumulative distribution curves of zenith delay RMS for the KSC STI (warmer months shown in reddish curves, winter months in bluish/purplish curves).

5. CONCLUSION

Remote sensing in meteorology is normally thought of as being done from satellites. However, ground-based remote sensing is also important in operational meteorology. As is described, ground-based remote sensing is critical to the success of America's space program at NASA's Kennedy Space Center and Cape Canaveral Air Force Station in Florida. In addition, the Ka Band Object Observation and Monitoring project, which is a unique application of remote sensing being developed to improve capability for tracking space debris and near Earth asteroids will become more important as future satellites are deployed and greater use is made of Low Earth Orbit (LEO). Site Test Interferometers, which will allow for scheduling observations to minimize atmospheric degradation on the project's operations is an example of the emerging ground based technology that will support and enhance future remote sensing capabilities.

REFERENCES

- [1] Boyd, B. F., Madura, J. T., and Adams, M. E., "Meteorological support to the United States Air Force and NASA at the Eastern Range and Kennedy Space Center," Paper 93-0753, *AIAA 31st Aerospace Sciences Meeting and Exhibit*, (January 1993).
- [2] Hazen, D. S., Roeder, W. P., Boyd, B. F., Lorens, J. B., and Wilde, T. L., "Weather impact on launch operations at the Eastern Range and Kennedy Space Center," *Preprints, Sixth Conf. on Aviation Weather Systems, Amer. Meteor. Soc.*, pp. 270-275. (1995).
- [3] Krider, E. P., Koons, H. C., Walterscheid, R. L., Rust, W. D., and Willett, J. C., "Natural and triggered lightning launch commit criteria (LCC)," *Aerospace Report No. TR-99(1413)-1*, 15 January 1999.
- [4] Krider, E. P., Christian, H. J., Dye, J. E., Koons, H. C., Madura, J. T., Merceret, F. J., Rust, D. L., Walterscheid, R. L., and Willett, J. C., "Natural and triggered lightning launch commit criteria (LCC)," *Conference on Aviation, Range and Aerospace Meteorology*, (2006).
- [5] McNamara, T. M., Roeder, W. P., and Merceret, F. J., "The 2009 update to the lightning launch commit criteria," *14th Conference on Aviation, Range, and Aerospace Meteorology*, (2010).
- [6] Roeder, W. P., Hajek, D. L., Flinn, F. C., Maul, G. A., and Fitzpatrick, M. E., "Meteorological and oceanic instrumentation at Spaceport Florida - opportunities for coastal research," *5th Conference on Coastal Atmospheric and Oceanic Prediction and Processes*, (2003).
- [7] Boyd, B. F., Roeder, W. P., Lorens, J. B., Hazen, D. S., and Weems, J., "Weather Support to Pre-launch operations at the Eastern Range and Kennedy Space Center," *Preprints 6th Conference on Aviation Weather Systems*, pp. 135-140, (1995).
- [8] Walterscheid, R. L., Willett, J. C., Krider, E. P., Gelinias, L. J., Law, G. W., Peng, G. S., Seibold, R. W., Simmons, F. S. and Zittel, P. F., "Triggered lightning risk assessment for reusable launch vehicles at four regional spaceports," *Aerospace Report No. ATR-2010(5387)-1*, (30 April 2010).
- [9] Willett, J.C., Merceret, F. J., Krider, E. P., Dye, J. E., O'Brien, T. P., Rust, W. D., Walterscheid, R. L., Madura, J. T., and Christian, H. J., "Rationales for the Lightning Flight Commit Criteria," NASA/TM-2010-216291, 236 pp. (2010).
- [10] Roeder, W. P., "Lightning has fallen to third leading source of U.S. storm deaths," *2012 Annual Meeting of the National Weather Association*, (2012).
- [11] Barbré, R.E., "Characteristics of the Spliced KSC Doppler Radar Wind Profiler Database". Jacobs ESSSA Group Analysis Report. ESSSA-FY13-1935.
- [12] Boyd, B. F., Harms, D. E., Fitzpatrick, M. E., Stout, R. P., Rosati, P. N., Berlinrut, D. D., Parks, C. R., and Overbeck, K. B., "Weather Support To Range Safety," Joint Army Navy NASA Air Force Safety & Environmental Protection Subcommittee, CPIA Pub. 687, Vol. I, pp. 59-69. (1999).
- [13] Boyd, B. F., Harms, D. E., Rosati, P. N., Parks, C. R., and Overbeck, K. B., "Weather Support To Range Safety For Forecasting Atmospheric Sonic Propagation," *9th Conference on Aviation, Range, and Aerospace Meteorology*, pp. 432-437. (2000).
- [14] Harms, D.E., Boyd, B. F., Flinn, F. C., McNamara, T. M., Madura, J. T., Wilfong, T. L., and Conant, P. R., "Weather system upgrades to support space launch at the Eastern Range and Kennedy Space Center." *12th Symposium on Meteorological Observations and Instrumentation*, (2003).
- [15] Huffines, G. R. and Orville, R. E., "Lightning ground flash density and thunderstorm duration in the continental United States: 1989-96," *Journal of Applied Meteorology*, 38, 1013-1019 (1999).
- [16] Roeder, W.P. and Saul, J. M., 2012. "Four Dimensional Lightning Surveillance System: Status and Plans," 22nd International Lightning Detection Conference, (2012).
- [17] Roeder, W. P., "The Four Dimensional Lightning Surveillance System," *21st International Lightning Detection Conference*, (2010).
- [18] Cummins, K. L., Cramer, J. A., Biagi, C. J., Krider, E. P., Jerauld, J., Uman, M. A., Rakov, V. A., "The U.S. National Lightning Detection Network: Post upgrade status," *2nd conference on Meteorological Applications of Lightning Data*, (2006).
- [19] Roeder, W.P., McNamara, T. M., Boyd, B. F., and Merceret, F. J., "The new weather radar for America's space program in Florida: an overview," *34th Conference on Radar Meteorology*, (2009).
- [20] Roeder, W.P., T.M. McNamara, T. M., B.F. Boyd, B. F., J.W. Weems, J. W., and S.B. Cocks, S. B., "Unique uses of weather radar for space launch". *32nd Conference on Radar Meteorology*, (2005).

- [21] Thurmond, K. R., "Operational cloud-to-ground lightning forecasting utilizing S band dual-polarization radar," M.S. thesis, Air Force Institute of Technology, Wright-Patterson Air Force Base, OH, AFIT-ENP-14-M-36, 72 pp. (2014).
- [22] Woodard, C. J., Carey, L. D., Petersen, W. A., and Roeder, W. P., "Operational utility of dual-polarization variables in lightning initiation forecasting," *Electronic Journal of Operational Meteorology*, **13** (6), 79-102, (2012)
- [23] Ryzhkov, A. V., Schuur, T. J., Burgess, D. W., and Zrnic, D. S., 2005: Polarimetric tornado detection, *Journal of Applied Meteorology*, **44**, 557-570 (2005).
- [24] McLaughlin, S. and Wilfong, T. L., "NASA 49.25 MHz and NWS 449 MHz Radar Wind Profilers," Presentation given at the March 19-20, 2014 Day of Launch Working Group (DOLWG) meeting, Kennedy Space Center, FL, (March 2014).
- [25] Eastern Range Instrumentation Handbook, "Eastern Range Instrumentation Handbook," (CDRL B312), Systems Engineering and Analysis, Computer Sciences Raytheon, Patrick AFB, FL 32925, Contract FA2521-07-C-0011, (2012).
- [26] Geldzahler, B.J., "Coherent uplink arraying techniques for next generation orbital debris, near earth object, and space situational awareness radar systems," *Proc. SPIE 8382, Active and Passive Signatures III*, (2012).
- [27] Yeomans, D., "Near Earth Object Program," NASA Jet Propulsion Laboratory, 7 July 2014, <<http://neo.jpl.nasa.gov/neo/>> (14 July 2014).
- [28] Shambayati, S., Border, J. S., Morabito, D. D., and Mendoza, R., "MRO Ka-band demonstration: cruise phase lessons learned," IEEE Aerospace Conference, pp.1-17. (2007).
- [29] Geldzahler, B. J., Seibert, M. A., Miller, M. J., Vlnrotter, V., and Tsao, P., "KaBOOM - Band Objects: Observation and Monitoring," Advanced Maui Space Surveillance and Optical Technologies Conference, (2012).
- [30] Vlnrotter, V., Lee, D., Cornish, T., Tsao, P., Paal, L., and Jamnejad, V., "Uplink Array Concept Demonstration with the EPOXI Spacecraft," IEEE Aerospace Conference, (2009).
- [31] D'Addario, L., R. Proctor, J. Trinh, E. Sigman, and C. Yamamoto, "Uplink Array Demonstration With Ground-Based Calibration," Interplanetary Network Progress Report, Vol 42-176. <http://ipnpr.jpl.nasa.gov>. (2009).
- [32] Martin, P., Minear, K., Geldzahler, B., and Soloff, J., "Large Reflector Uplink Arraying," SpaceOps 2010 Conference, (2010).
- [33] Morabito, D.D., D'Addario, L. R., Acosta, R. J., and Nessel, J. A., "Tropospheric delay statistics measurement by two site test interferometers at Goldstone, California," *Radio Science* **48**, 1-10 (2013).
- [34] Morgan, J. G. and Morabito, D. D., "Implementation of the site test interferometer (STI) at KSC", KaBOOM Memo No. 7, pp. 1-11, (December 2013).

APPENDIX A – LIST OF ACRONYMS

3-D	three dimensional	LCC	Launch Commit Criteria
45WS	45th Weather Squadron	LDAR	Lightning Detection and Ranging
4DLSS	Four Dimensional Lightning Surveillance System	LO	local oscillator
AFB	Air Force Base	LPLWS	Launch Pad Lightning Warning System
CCAFS	Cape Canaveral Air Force Station	m	meter
CfA	Center for Astrophysics	MERLiN	Mesoscale Eastern Range Lightning Network
CGLSS	Cloud-to-Ground Lightning Surveillance System	MHz	megahertz
cm	centimeter	MSFC	Marshall Space Flight Center
DoD	Department of Defense	NASA	National Aeronautics and Space Administration
DRWP	Doppler Radar Wind Profiler	NE	Natural Environments
DSN	Deep Space Network	NEO	Near-Earth Object
ER	Eastern Range	NEXRAD	Next Generation Weather Radar
FAA	Federal Aviation Administration	NLDN	National Lightning Detection Network
GHz	gigahertz	NM	nautical mile
HQ	Headquarters	NWS	National Weather Service
IF	intermediate frequency	ps	picosecond
JPL	Jet Propulsion Laboratory	RMS	root mean square
KaBOOM	Ka band Objects Observation and Monitoring	s	second
kft	kilofeet	STI	Site Test Interferometer
km	kilometer	U.S.	United States
KSC	Kennedy Space Center	USAF	United States Air Force
kV/m	kilovolts per meter	VAD	Velocity Azimuth Display
kW	kilowatt	VHF	very high frequency
LEO	Low Earth Orbit	WSR-88D	Weather Surveillance Radar 1988 Doppler